



Original Article

## Comparison between half-cell potential of reinforced concrete exposed to carbon dioxide and chloride environment

Kitipoom Chansuriyasak<sup>1</sup>, Chalermchai Wanichlamlart<sup>2</sup>, Pakawat Sancharoen<sup>2</sup>,  
Waree Kongprawechnon<sup>3</sup> and Somnuk Tangtermsirikul<sup>1,2</sup>

<sup>1</sup> School of Civil Engineering and Technology,

<sup>2</sup> Construction and Maintenance Technology Research Center (CONTEC),

<sup>3</sup> School of Information, Computer, and Communication Technology,  
Sirindhorn International Institute of Technology, Thammasat University, Khlong Luang, Pathum Thani, 12120 Thailand.

Received 25 December 2009; Accepted 3 August 2010

### Abstract

The objective of this study is to investigate the effect of concrete mix proportion and fly ash on half-cell potential (HCP) and corrosion current density ( $i_{corr}$ ) of steel in concrete exposed to different environments. Reinforced concrete specimens with different fly ash replacement percentages and water to binder ratios (w/b) were studied in this paper. The specimens were subjected to two highly corrosive environments which are chloride and carbon dioxide. HCP and  $i_{corr}$  were used to monitor the corrosion process. Results of this study demonstrate that both HCP and  $i_{corr}$  indicated the same tendency, especially for corroded specimens after being exposed to chloride. This means that HCP can be used to inspect corrosion of steel due to chloride. In case of carbonation, concrete specimens with fly ash showed more negative potential values than concrete without fly ash. However, chloride exposure test exhibited that specimen with higher fly ash replacement corroded earlier. Moreover, HCP measurement presented different values between concrete exposed to chloride and carbon dioxide. There was an effect of carbonation to increase HCP during the initiation stage. A proper evaluation guideline for steel corrosion due to carbonation needs to be further studied.

**Keywords:** corrosion, half-cell potential, non-destructive test, chloride, carbonation, inspection

### 1. Introduction

Corrosion of reinforcing steel is a major type of deterioration in reinforced concrete structures. Products of corrosion exhibit volume expansion and induce tensile stress in concrete, which ultimately result in cracking and spalling of concrete cover. Due to loss of steel cross-section and covered concrete, there could be a significant reduction in load bearing capacity of the structures. It is well known that

steel reinforcement in concrete is protected from corrosion by a passive film formed due to the high alkalinity of concrete. A passive film of hydrated iron oxide with a thickness of a few atomic layers is created on the steel surface. This passive film is decomposed due to penetration of chloride ions ( $Cl^-$ ) or carbon dioxide ( $CO_2$ ). Mechanisms of corrosion begin when ferrous ions ( $Fe^{2+}$ ) from anode are dissolved and electrons are set free. These electrons drift through the steel to the cathode, where, together with the generally available water and oxygen, they form hydroxide ( $OH^-$ ). However, many reports (Gu and Beaudoin, 1998; Elsener, 2001; Sancharoen *et al.*, 2009) show different corrosion mechanisms of steel in concrete when subjected to chloride and

\* Corresponding author.  
Email address: kitipoomc@gmail.com

carbon dioxide. In the case of carbonation, anode and cathode areas cannot be localized as they are very small in size and are evenly distributed. On the other hand, corrosion of steel in concrete due to chloride shows much smaller anode area than that of the cathode and both can be far away from each other. Corrosion inspection of steel can be conducted by many different techniques. Non-destructive techniques such as half-cell potential measurement (HCP) and corrosion current density ( $i_{corr}$ ) are two well known techniques (Pradhan and Bhattacharjee, 2009).

Corrosion of steel can be investigated by HCP measurement according to ASTM C876 via an electrochemical process. If a steel bar is depassivated, electrons flow from the steel bar to the reference half cell (usually a copper rod). At the reference half cell, electrons would be consumed in a reduction reaction, transforming copper ions in the copper sulfate solution into copper atoms deposited on the rod. A voltmeter is connected to the electrical circuit to measure the reference potential as shown in Figure 1. The voltmeter usually indicates a negative value during the measurement. The value of the potential is used as an indicator of the likelihood of corrosion activity as shown in Table 1 (ASTM C876), for a Cu/CuSO<sub>4</sub> electrode. If the potential is more than -200 mV, there is a high possibility that no corrosion is occurring at the time of measurement. If the potential is less than -350 mV, there is a high possibility of active corrosion.

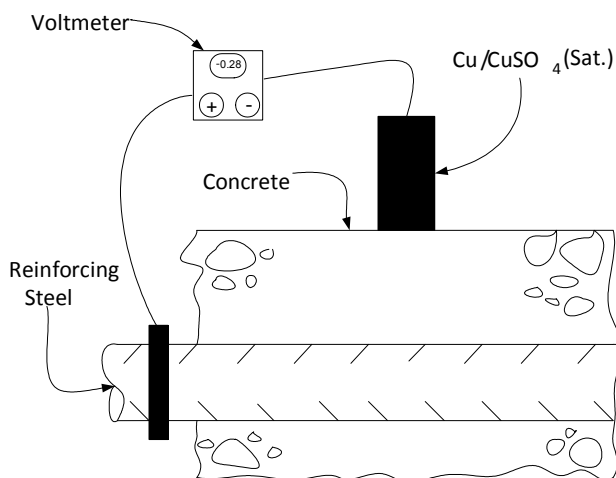


Figure 1. Schematic illustration of the half-cell potential measurement

Table 1. Interpretation guideline of half-cell potential measurement based on ASTM C876

Half-cell potential, mV <sup>a</sup>	Corrosion interpretation
>-200	Low probability of corrosion
-200 to -350	Corrosion activity uncertain
<-350	High probability of corrosion

<sup>a</sup>Measurements made with a Cu/CuSO<sub>4</sub> electrode

Corrosion possibility is uncertain when the voltage is in the range of -200 to -350 mV. However, RILEM TC 153-EMC suggests that numerical criteria given by ASTM C 876 lead to misinterpretation because measured values of the potential fluctuate upon various factors such as mix proportion of concrete, type of ingredients, cover thickness of reinforcing steel, moisture content inside the concrete and type of corrosion of reinforcing steel. In addition, as carbonation process leads to an increase of concrete resistivity, HCP values tend to be less negative on both passive and corroding reinforcing steels. When concrete cover thickness is increased, the difference between active and passive potential values is diminished, resulting in a uniform potential value at infinite. Thus, locations of localised corrosion become more difficult to be detected when cover depth is increased (Hansson *et al.*, 2006; Elsener, 2002; Andrade and Alonso, 1996). Moisture condition of concrete also affects resistivity of concrete. Changes in moisture content may lead to a difference of potentials up to 200 mV (Gu and Beaudoin, 1998). It is important to consider not only the difference of moisture condition at a measuring point but also variation along the whole structure. HCP values become more negative as concrete moisture increases (RILEM TC 154-EMC, 2003). Moreover, concrete normally used in construction has large variety in mix proportion as well as type of cementitious materials. The effect of fly ash widely used as partial cement replacement material in Thailand on HCP measurement has not been clarified yet.

The main objective of this study is to investigate the effect of different corrosive environments i.e. carbon dioxide and chloride, on half-cell potential and corrosion current density. Concrete specimens were prepared with different cover thickness, percentage of fly ash replacement, and w/b ratio. The effects of these variables on HCP and  $i_{corr}$ , used to investigate steel corrosion due to chloride and carbon dioxide, were studied.

## 2. Experimental program

### 2.1 Materials and concrete mix proportions

Ordinary Portland Cement (Type I) was used in this study. Fly ash type F according to ASTM C618 (type 2b according to Thai Industrial Standard, TIS 2135) was used as a partial cement replacement material for producing fly ash concrete specimens. Chemical compositions and physical properties of the cement and fly ash are given in Table 2. Crushed limestone with a maximum size of 19 mm was used as coarse aggregate. Fine aggregate was river sand with fineness modulus of 3.12. Both aggregates complied with the requirements of ASTM C33. Void content of the compacted mixtures of fine and coarse aggregates was tested according to ASTM C29/C29M. The sand to total aggregate ratio of 0.45, with a minimum void ratio of 0.23, was used in all concrete mix proportions. Nine different concrete mix proportions were prepared for this study as shown in Table 3.

Table 2. Chemical compositions and physical properties of ordinary Portland cement and fly ash

Material	SiO <sub>2</sub> (%)	Al <sub>2</sub> O <sub>3</sub> (%)	Fe <sub>2</sub> O <sub>3</sub> (%)	CaO (%)	MgO (%)	SO <sub>3</sub> (%)	LOI <sup>a</sup> (%)	BF <sup>b</sup> (cm <sup>2</sup> /g)	Specific gravity
Cement	20.48	5.25	3.82	65	0.95	0.01	1.17	3350	3.15
Fly ash	43.88	24.31	12.51	11.18	2.75	0.78	0.17	3460	2.08

<sup>a</sup>Loss on ignition<sup>b</sup>Blaine fineness

Table 3. Mix proportions of tested concrete

No.	Designation	w/b	Cement (kg/m <sup>3</sup> )	Fly ash (kg/m <sup>3</sup> )	Water (kg/m <sup>3</sup> )	Fine aggregate (kg/m <sup>3</sup> )	Coarse aggregate (kg/m <sup>3</sup> )
1	0.4C100	0.4	454	0	182	720	1032
2	0.4C80FA20	0.4	348	87	174	720	1032
3	0.4C50FA50	0.4	204	204	163	720	1032
4	0.5C100	0.5	399	0	199	720	1032
5	0.5C80FA20	0.5	307	77	192	720	1032
6	0.5C50FA50	0.5	181	181	181	720	1032
7	0.6C100	0.6	355	0	213	720	1032
8	0.6C80FA20	0.6	274	69	206	720	1032
9	0.6C50FA50	0.6	163	163	196	720	1032

## 2.2 Specimen preparation

Deformed bars having grade SD40 according to TIS 24 with nominal diameter of 12 mm and length of 310 mm were used as reinforcing steels. They were polished using a wire brush to remove rust shown on the surface and then degreased by acetone. All steel bars were wrapped by insulating tape on both ends so that 210 mm center portion of the bar is exposed. Both tape-insulated ends of the steel bars were coated again by epoxy as shown in Figure 2.

Shape of specimens used for chloride exposure was modified from ASTM G109 as shown in Figure 3. Specimen prismatic dimensions are 95 mm × 200 mm × 250 mm. Cover thickness of the top reinforcing bar was varied as 30 mm and 50 mm. Two bottom reinforcing bars were placed 80 mm below the top bar and were used as reference bars. The top and bottom bars were electrically connected with lead wires and a 100 Ω resistor.

Dimensions of prism specimens exposed to carbon dioxide are 200 mm × 200 mm × 250 mm. Concrete cover of steel was varied as 20 mm, 30 mm, 40 mm and 50 mm. At the center of each specimen, a reference bar was placed. Each reinforcing bar was electrically connected to the reference bar by lead wires and a 100 Ω resistor as shown in Figure 4.

## 2.3 Exposure conditions

All specimens were demolded 24 hours after casting and were cured by covering with wet clothes for another 27

days in a laboratory atmosphere. After removing from the curing room, the specimens were immediately exposed to test conditions. Two conditions of exposure were applied. In case of carbonation, carbon dioxide concentration in the carbonation chamber was kept at 4%. The temperature and relative humidity were controlled at 40°C and 55%, respectively. This

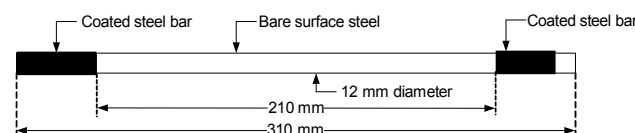


Figure 2. Steel bar coating arrangements

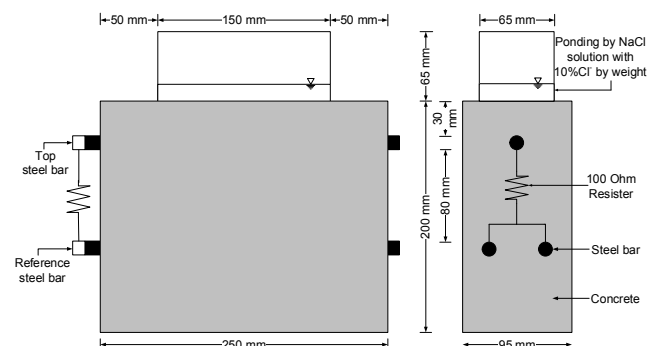


Figure 3. Schematic illustration of specimen exposed to chloride

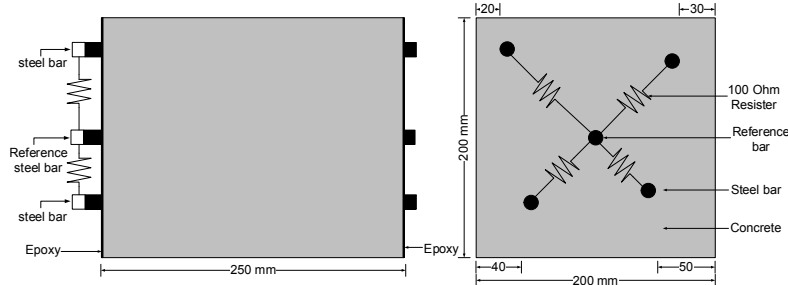


Figure 4. Schematic illustration of specimen exposed to carbonation

test condition was selected to accelerate the process of carbonation. The second set of specimens was exposed to sodium chloride solution of which the chloride concentration was 10% by weight of the solution. This solution was used as the continuously ponding solution above the top surface of all specimens.

## 2.4 Test methods

### 2.4.1 Half-cell potential measurement

The corrosion potential of reinforcing steels was measured by means of HCP measurement. The HCP value indicates the probability of corrosion activity of the reinforcing steel located beneath the half cell, as described by ASTM C 876. The setup basically consists of an external copper/copper sulfate ( $\text{Cu}/\text{CuSO}_4$ ) electrode (half cell), connecting wires and a high impedance voltmeter. The half-cell potential measurement has been widely used in the field due to its simplicity and general agreement among researchers that it effectively indicates the probability of active corrosion along the steel reinforcement in concrete. In case of chloride exposure, specimens were air-dried for one hour before the HCP measurement. In case of carbonation, specimens were wetted by covering with wet clothes for twelve hours to increase the moisture in concrete because environment in the carbonation chamber was usually very dry. The reference electrode was a copper/saturated copper sulfate electrode ( $\text{Cu}/\text{CuSO}_4$ ). Measurement was conducted on the top surface at every 20 mm along the direction of top reinforcing bar. HCP was measured every day in case of chloride exposure and every week for carbon dioxide exposure.

### 2.4.2 Corrosion current density

Normally, corrosion will be firstly initiated as microcell corrosion between anode and cathode within the top reinforcing bar. However, measurement of microcell corrosion current is very difficult because the area of anode and cathode are very small. In case of macrocell corrosion, the area of anode is smaller than that of the cathode. Thence, it can evaluate a corrosion status easier than microcell corrosion as recommended by ASTM G109. In this study, only

macrocell corrosion current was measured. Macrocell corrosion current is a good indicator of corrosion initiation of the reinforcing steel. Corrosion current ( $I$ ) was measured indirectly as a voltage drop across the 100  $\Omega$  resistor connected externally between the top and bottom reinforcing bars. The corrosion current is calculated based on Ohm's law as shown in Eq (1).

$$V = IR \quad (1)$$

where  $V$  is the voltage drop across the resistor ( $\mu\text{V}$ ),  $I$  is the current ( $\mu\text{A}$ ),  $R$  is the electrical resistance (100  $\Omega$  in this study). Voltmeter is of a high impedance type with a resolution of 0.01 mV as recommended by ASTM G109. Then, corrosion current density ( $i_{corr}$ ) was calculated as shown in Eq (2).

$$i_{corr} = \frac{I}{A} \quad (2)$$

where  $i_{corr}$  is the corrosion current density ( $\mu\text{A}/\text{cm}^2$ ), and  $A$  is the surface area of exposed reinforcing steel. In this study, exposed steel has the surface area of 79.168  $\text{cm}^2$  (surface area of the center portion without epoxy coat).

### 2.4.3 Determination of chloride content

Total chloride contents in concrete were determined according to ASTM C1152 after the specimens has been ponded for 36 days. Five grams of powdered concrete at the surface of reinforcing bar was collected. Then, the sample of powdered concrete was dissolved in  $\text{HNO}_3$  (nitric acid) solution, and titrated against N/20  $\text{AgNO}_3$  (silver nitrate) solution. Total chloride content was calculated as percentage of chloride ion by weight of the powder sample.

### 2.4.4 Carbonation depth measurement

Accelerated carbonation test was conducted. Concrete specimens with the size of 100×100×600 mm were used for carbonation test. At 24 hours after casting, the specimens were demolded and moisture-cured for 27 days. On the 28<sup>th</sup> days, specimens were exposed to carbon dioxide in the carbonation chamber. At the age of carbonation depth

measurement, specimens were split and cleaned to remove dust from the fresh surface. The depths of carbonation were determined by spraying on a freshly broken surface with a phenolphthalein solution. The average carbonation depth was calculated from eight measurement points on every side of the specimen.

### 3. Results and Discussion

#### 3.1 Chloride environment

It is well known that corrosion current measurement according to ASTM G109 can be used to investigate corrosion initiation of steel effectively but it is difficult to be used in the field. In contrast, HCP measurement is popular for the field measurement. However, there are many parameters which affect HCP values according to ASTM C876. In this study, the results of HCP values were compared with  $i_{corr}$ . Figures 5(a) and 5(b) show the values of  $i_{corr}$  (top of left axis) and HCP (bottom of left axis) of the specimen with 30 mm concrete cover thickness exposed to chloride environment. After ponding for a period of time,  $i_{corr}$  rapidly increased, indicating depassivation of reinforcing steel. At the time when  $i_{corr}$  increased, HCP value also increased. This indicates that HCP is effective for detecting corrosion initiation of steel exposed to chloride. The value of the HCP was in the range of -200 to -600 mV. All potential values of concrete specimens become more negative after ponding for a certain period of the time which depends on the w/b ratio and percentage of fly ash. Figure 5(a) shows that HCP of specimen with 0.6 in w/b ratio and 50% in fly ash replacement dropped at very early day. After longer time of ponding, specimens with w/b 0.5 and 0.4 showed HCP drop along with increase in  $i_{corr}$  values. Subsequent ponding of all specimens showed constant HCP values at about -500 mV to -600 mV after 18 days which implied that corrosion was stabilized. Figure 5(b) demonstrates the effect of fly ash replacement percentage of concrete with w/b of 0.6. HCP and  $i_{corr}$  of concrete specimens with 50% fly ash replacement dropped firstly followed by those of the concrete specimen with 20% fly ash replacement and OPC concrete specimen. It is well known that potential values less than -350 mV indicate 90% probability of corrosion according to ASTM C876. Based on this criterion, specimen with 0.6 in w/b ratio showed high probability of corrosion after ponding for 4 days. Then, specimens with 0.4 and 0.5 in w/b ratios showed high probability of corrosion after ponding for 13 and 15 days, respectively. The trend of HCP drop was in line with that of the increase of  $i_{corr}$ . Moreover, the risk of corrosion of the steel was also verified by determining chloride content at steel surface (1 cm near the surface of steel bar) as shown in Figure 6. In case of specimen with 0.6 in w/b and 50% replacement of fly ash, total chloride content is 0.12% by weight of concrete, which is higher than the chloride content threshold to initiate corrosion. The chloride threshold is regulated according to EIT 1014 (Standard of the Engineering Institute of Thailand) as

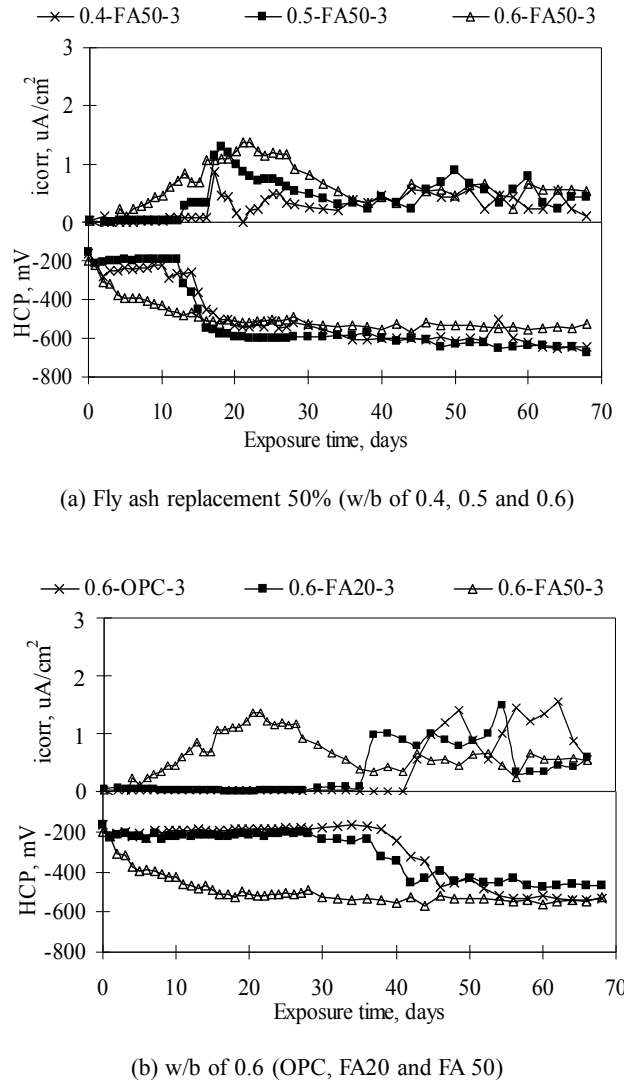


Figure 5. Relationship between HCP and  $i_{corr}$  values at different exposure time in chloride environment

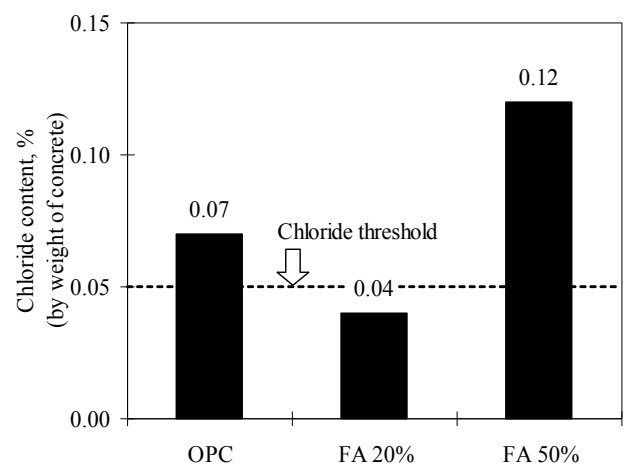


Figure 6. Total chloride content of specimen with w/b = 0.6 and differently ash content

0.4% of total binder which is approximately 0.05% by weight of the tested concrete sample.

It is widely known that fly ash can increase the resistance of concrete against chloride diffusion (Sumranwanich and Tangtermsirikul, 2004). However, result of total chloride content of specimen with 50% fly ash replacement showed a highest value as shown in Figure 6. This is because the specimen was exposed to chloride on the 28<sup>th</sup> day which is still young for high volume fly ash concrete. Pozzolanic reaction of fly ash in the concrete had not proceeded much especially when fly ash was used in a large content, so the porosity of the concrete with 50% fly ash replacement could be higher than those of other specimens (Maruya *et al.*, 2003; Sumranwanich and Tangtermsirikul, 2004). Chloride content of specimen with 0% fly ash was higher than the chloride threshold but HCP still showed no corrosion. This could be due to effect of  $\text{Cl}/\text{OH}^-$  ratio. The passive film surrounding the steel bar was destroyed due to chloride ions. However, since pH of the OPC concrete was high, the steel bar might not yet start to corrode (Thangavel and Rengaswamy, 1998). In case of OPC concrete, the amount of OH is higher than that of the fly ash concrete. Future studies are needed to verify the effect of alkalinity on the chloride threshold.

### 3.2 Carbon dioxide environment

In the case of specimens exposed to carbon dioxide, Figures 7(a) and 7(b) demonstrate the effects of water to binder and percentage of fly ash replacements on HCP and  $i_{\text{corr}}$ , respectively. The results of HCP of all specimens exposed to carbon dioxide environment showed less negative value when exposure time increased as shown in Figures 7(a) and 7(b). However, the  $i_{\text{corr}}$  of all specimens were constant. This means that corrosion of steel had not yet been initiated then. This can be verified by results of carbonation depth as shown in Figure 8. All carbonation depths had not yet reached the steel surface. For example, the specimen with 0.4 w/b ratio and 50% fly ash replacement showed smaller depth of carbonation (5.5 mm) than the concrete cover thickness (30 mm). Concrete specimens with higher w/b ratio showed larger depth of carbonation. Similarly, specimens with higher replacement ratio of fly ash showed higher depth of carbonation. These results get along with typical trends of carbonation (Khunthongkeaw *et al.*, 2006).

### 3.3 Comparison between HCP values measured in chloride and carbon dioxide environments

Figures 9(a) and 9(b) illustrate comparison between effects of chloride and carbon dioxide environments on HCP values. Figure 9(a) shows HCP values in chloride environment. The HCP values were constant up to corrosion initiation time. After corrosion, HCP decreased rapidly to more negative values. On the other hand, HCP increased to less negative values after specimens were exposed to carbon di-

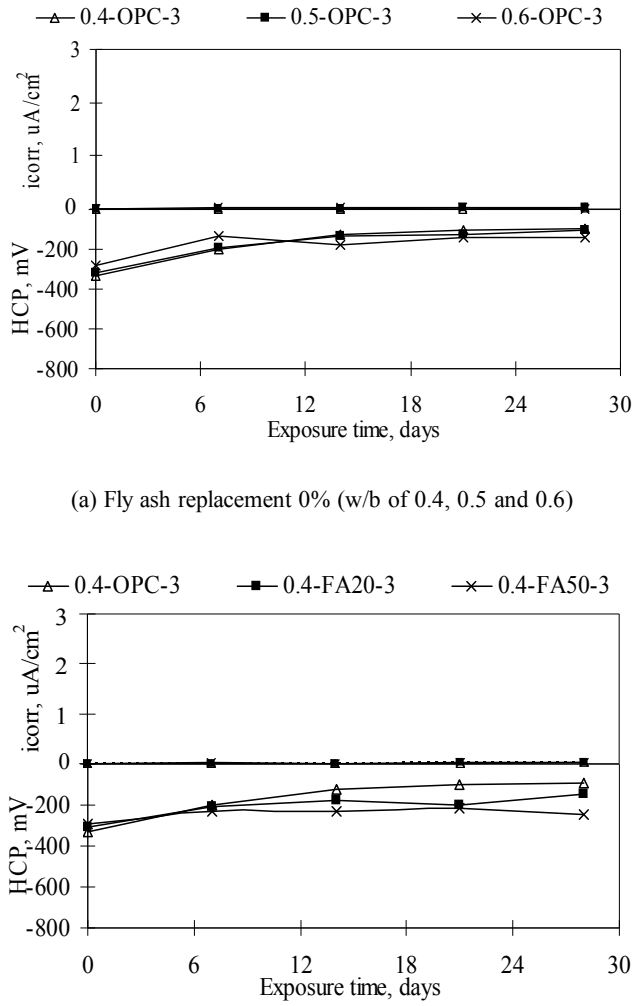


Figure 7. Relationship between HCP and  $i_{\text{corr}}$  values at different exposure time in carbon dioxide

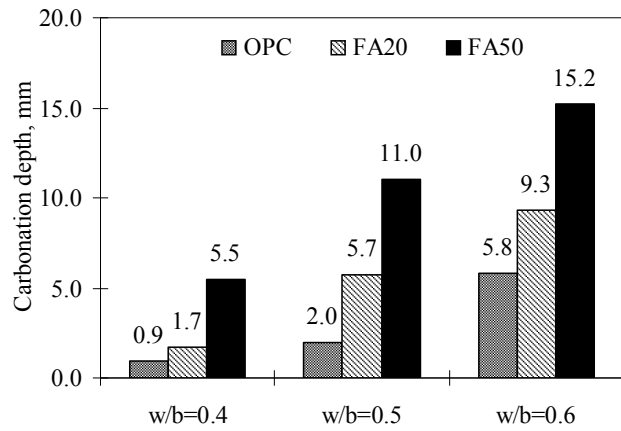


Figure 8. Carbonation depth of concrete after being exposed for 28 days

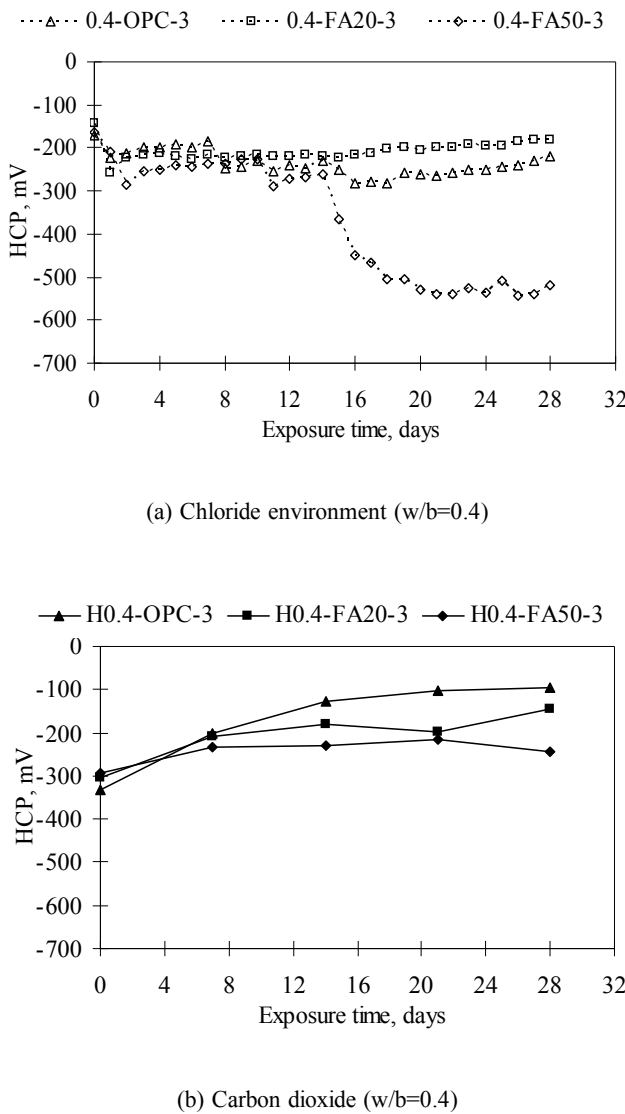


Figure 9. HCP measurement of specimens exposed to chloride environment and carbon dioxide

oxide as shown in Figure 9(b). These results showed similar tendency with the results by V.Zivica (2003) which reported effect of carbonation on HCP measurement. The HCP showed less negative values due to increasing electrical resistance of concrete by carbonation. Because carbonation leads to a significant reduction in the permeability and porosity of concrete, Calcium carbonates which is produced from carbonation reaction fill in the pores of the structure and increase the electrical resistance of concrete. Thus, the electrical current of the HCP device was reduced. This summary was in accordance to the report by Chi (2002) which presented the effect of carbonation on permeability and porosity of concrete, and in RILEM TC 154-EMC, 2003 which presented the effect of resistivity of concrete on HCP values. However, the effect of carbonation on HCP and  $i_{corr}$  after a steel reinforcement has been depassivated needs to be further studied.

#### 4. Conclusions

From the experimental results, following observations/conclusions can be drawn:

1. Half-cell potential values and corrosion current density values showed similar trends, especially after corrosion was initiated. Half-cell potential measurement can be used to detect corrosion initiation of reinforcing bars.

2. The HCP values were dependent on concrete exposure conditions. For chloride environment, HCP values were constant before corrosion initiation time. After the steel was depassivated, HCP rapidly decreased to more negative values. However, for carbonation, HCP values increased to be less negative due to increasing resistance of carbonated concrete.

3. It has been widely known that fly ash concrete shows better resistance against chloride environment. However, in this study, 50%FA specimen showed earlier depassivation. This can be verified by the results of chloride content in which 50%FA specimen had higher chloride content near the steel surface than the critical chloride content, whereas 20%FA and 0%FA specimens exhibited lower than critical contents. This was due to the effect of curing condition on chloride penetration resistance (HCP also showed no depassivation for 20%FA and 0%FA). Further studies are needed to clarify the effect of alkalinity on chloride threshold.

#### References

- Andrade, C. and Alonso, C. 1996. Corrosion rate monitoring in laboratory and on-site, *Construction and Building Materials*. 10, 315-328.
- ASTM C1152. 1997. Standard test method for acid-soluble chloride in mortar and concrete, *Annual Book of ASTM Standards*, Vol.14.02.
- ASTM C29. 1997. Standard test method for bulk density ("Unit Weight") and voids in aggregate, *Annual Book of ASTM Standards*, Vol.14.02.
- ASTM C33. 1999. Standard specification for concrete aggregates, *Annual Book of ASTM Standards*, Vol.14.02.
- ASTM C876. 1999. Standard test method for half-cell potentials of uncoated reinforcing steel in concrete, *Annual Book of ASTM Standards*, Vol.14.02.
- ASTM C618. 1999. Standard specification for coal fly ash and raw or calcined natural pozzolan for use as a mineral admixture in concrete, *Annual Book of ASTM Standards*, Vol.14.02.
- ASTM G109. 1999. Standard test method for determining the effects of chemical admixtures on the corrosion of embedded steel reinforcement in concrete exposed to chloride environments, *Annual Book of ASTM Standards*, Vol.3.02.
- EIT 1014-40. 1997. Specification and standard of materials and construction for reinforced concrete design, *Engineering Institute of Thailand Under H.M. The King's Patronage*.

Elsener, B. 2001. Half-cell potential mapping to assess repair work on RC structures, *Construction and Building Materials.* 15, 133-139.

Elsener, B. 2002. Macrocell corrosion of steel in concrete – implications for corrosion monitoring. *Cement and Concrete Composites.* 24, 65-72.

Gu, P. and Beaudoin, J.J. 1998. Obtaining effective half-cell potential measurement in reinforced concrete structure, *Institute for research in construction*, 1-4.

Hansson, C.M., Poursaei, A. and Laurent, A. 2006. Macrocell and microcell corrosion of steel in ordinary Portland cement and high performance concrete, *Cement and Concrete Research.* 36, 2098-2102.

Khunthongkeaw, J., Tangtermsirikul, S. and Leelawat, T. 2006. A study on carbonation depth prediction for fly ash concrete, *Construction and Building Materials.* 20, 744-753.

Maruya, T., Hsu, K., Takeda, H. and Tangtermsirikul, S. 2003. Numerical modeling of steel corrosion in concrete structure due to chloride ion oxygen and water movement, *Journal of Advanced Concrete Technology.* 1, 147-160.

Pradhanl, B. and Bhattacharjee, B. 2009. Half-cell potential as an indicator of chloride-induced rebars corrosion initiation in RC, *Journal of Materials in Civil Engineering, ASCE.* 21, 542-542.

RILEM TC 154-EMC. 2003. Half-cell potential measurements – Potential mapping on reinforced, Concrete Structures, Materials and Structures. 36, 461-471.

Sancharoen, P., Tsai, S.H., Tangmitoracha, J. and Tangtermsirikul, S. 2009. Application of half-cell potential measurement to inspect corrosion of reinforcing steel, *Proceedings of the 14<sup>th</sup> Thailand National Convention on Civil Engineering, Thailand.*

Sumranwanich, T. and Tangtermsirikul, S. 2004. A model for predicting time-dependent chloride binding capacity of cement-flyash cementitious system, *Materials and Structures.* 37, 387-396.

TIS 24. 2005. Steel bars for reinforced concrete: deformed bars, *Ministry of Industry, Thailand.*

TIS 2135. 2002. Coal fly ash for use as an admixture in concrete, *Ministry of Industry, Thailand.*

Thangavel, K. and Rengaswamy, N.S. 1998. Relationship between chloride/hydroxide ratio and corrosion rate of steel in concrete, *Cement and concrete Composites.* 20, 283-292.

Zivica, V. 2003. Corrosion of reinforcement induced by environment containing chloride and carbon dioxide, *Bulletin of Material Science,* 26, 605-608.